# Simultaneous radar observations of meter-scale *F* region irregularities at and off the magnetic equator over India

A. K. Patra,[1] D. Tiwari,[2,3] S. Sripathi,[1,3] P. B. Rao,[4] R. Sridharan,[2] C. V. Devasia,[2] K. S. Viswanathan,[2] K. S. V. Subbarao,[2] R. Sekar,[5] and E. A. Kherani[5,6]

Received 28 April 2004; revised 8 November 2004; accepted 22 December 2004; published 19 February 2005.

[1] Simultaneous observations of equatorial spread *F* irregularities made with an 18 MHz radar from Trivandrum, located at the geomagnetic equator, and a 53 MHz radar from Gadanki, located at a magnetic latitude of 6.5°N, corresponding to nearly the same longitude zone, are presented. The observations correspond to 8.3 and 2.8 m irregularities, respectively. The spread *F* irregularities at both the locations are found to occur nearly at the same time but are observed for longer duration at Gadanki than at Trivandrum. The spread *F* structures as observed in the intensity maps corresponding to Gadanki are characterized by multiple periodic plumes in contrast to a limited number of plumes observed over Trivandrum. The Doppler velocities associated with these irregularities corresponding to Trivandrum are in the range of $-100$–$150$ m s$^{-1}$, whereas they are in the range of $-100$–$250$ m s$^{-1}$ at Gadanki. Further, the fluctuating velocity fields are much stronger in the Gadanki observations than in the Trivandrum observations. Remarkably, the spectral widths are $<100$ m s$^{-1}$ in Trivandrum observations in contrast to those observed at Gadanki with values as high as 300 m s$^{-1}$. The observations are compared with those made elsewhere and are discussed in the light of current understanding of the meter-scale irregularities responsible for the radar backscatter.

**Citation:** Patra, A. K., D. Tiwari, S. Sripathi, P. B. Rao, R. Sridharan, C. V. Devasia, K. S. Viswanathan, K. S. V. Subbarao, R. Sekar, and E. A. Kherani (2005), Simultaneous radar observations of meter-scale *F* region irregularities at and off the magnetic equator over India, *J. Geophys. Res.*, *110*, A02307, doi:10.1029/2004JA010565.

## 1. Introduction

[2] The plasma irregularities in the equatorial *F* region manifest in the form of diffuse ionograms and are referred to as equatorial spread *F* (ESF) [*Berkner and Wells*, 1934; *Booker and Wells*, 1938]. ESF is now known to be a manifestation of ionospheric interchange instabilities like the Rayleigh-Taylor instability and the gradient drift instability responding to the steep density gradient in the nighttime equatorial *F* region. The general understanding is that, in the linear regime of these instabilities, only the bottom side of the *F* region becomes unstable and in the nonlinear regime, the depletion channels associated with these instabilities penetrate through the *F* region peak electron density well into topside. These channels are referred to as plasma bubbles and display plume-like structures in the radar backscatter map [*Woodman and LaHoz*, 1976]. The instability processes operating in the *F* region generate plasma density irregularities with scale sizes ranging from a few centimeters to hundreds of kilometers. These irregularities have been studied using coherent and incoherent scatter radars [*Woodman and LaHoz*, 1976; *Tsunoda et al.*, 1979; *Tsunoda*, 1980; *Towle*, 1980; *Hysell et al.*, 1994; *Hysell and Burcham*, 1998; *Hysell and Woodman*, 1997; *Patra et al.*, 1995; *Rao et al.*, 1997], radio beacons [*Krishnamoorthy et al.*, 1979; *Basu et al.*, 1988; *Chandra et al.*, 1993], rocket and satellite in situ instrumentation [*McClure et al.*, 1977; *Kelley et al.*, 1986; *Hanson and Bamgboye*, 1984; *Pfaff et al.*, 1997; *Sinha et al.*, 1999] and airglow [*Weber et al.*, 1978; *Sinha et al.*, 2001] as they are sensitive to different parts of the spectrum of the irregularities.

[3] Due to the high conductivity along the magnetic field lines, these structures are oriented along the geomagnetic north-south direction and are observed at all latitudes within about ±20°. *Weber et al.* [1978] have shown from airglow observations that these structures indeed map along the magnetic field lines. By using the ALTAIR incoherent scatter radar in the N-S scanning mode, *Tsunoda* [1980] has studied the N-S alignment of electron density structures associated with ESF. Using rocket data, *Vickrey et al.* [1984] have studied the mapping efficiency of the spread *F* structures along the magnetic field line. In this context, simultaneous observations of spread *F* irregularities made using any two radars operating from the same longitude but

[1]National MST Radar Facility, Tirupati, India.
[2]Space Physics Laboratory, Vikram Sarabhai Space Centre, Trivandrum, India.
[3]Now at Indian Institute of Geomagnetism, Navi Mumbai, India.
[4]National Remote Sensing Agency, Hyderabad, India.
[5]Physical Research Laboratory, Ahmedabad, India.
[6]Now at Instituto Nacional de Pesquisas Espaciais, São José dos Campos, Brazil.


0148-0227/05/2004JA010565

**Table 1.** Radar Specifications and Other Important Parameters Used for the Spread *F* Experiments at the Two Locations

| Parameter | Value | |
|---|---|---|
| | Trivandrum | Gadanki |
| Location | (77°E, 8.5°N, 0.5° dip) | (79.2°E, 13.5°N,12.5° dip) |
| Frequency, MHz | 18 | 53 |
| Peak transmitter power | 50 kW | 2.5 MW |
| Antenna | 12 × 6 dipole array | 32 × 32 three-element Yagi array |
| Antenna aperture, $m^2$ | $1.33 \times 10^4$ | $1.69 \times 10^4$ |
| Antenna gain, dB | 26.5 | 37 |
| Beam width | 6.3° in E-W | 2.8° in E-W |
| Beam direction | zenith | 14.8° off zenith due north |
| Receiver gain, dB | 110 | 120 |
| Receiver bandwidth | 80 KHz | 1.7 MHz |
| Receiver dynamic range, dB | 40 | 70 |
| Pulse width, μs | 100 | 16 |
| Interpulse period, ms | 10 | 4 |
| Number of FFT[a] | 256 | 256 |
| Number of spectral averaging | 16 | 8 |
| Height resolution, km | 15 | 4.8 |
| Velocity window, m $s^{-1}$ | ±415 | ±354 |
| Velocity resolution, m $s^{-1}$ | 3.25 | 2.76 |

[a]FFT: fast Fourier transform.

geomagnetically at different latitudes in the equatorial region connecting the *F* region field lines could be of significant value. Keeping this aspect in mind, we operated simultaneously a 18 MHz radar from Trivandrum (77°E, 8.5°N, dip angle 0.5°N), a magnetic equatorial location, and the 53 MHz MST radar from Gadanki (79.2°E, 13.5°N, dip angle 12.5°N), a low-latitude station, both located in the southern part of India. These two radars are sensitive to the Bragg scale sizes of 8.3 m and 2.8 m component of the electron density fluctuations respectively. In this paper, we present and discuss the simultaneous observations of ESF irregularities made on 12 nights during March–April 1998 and 1999 using the two radar systems from the equatorial station of Trivandrum and a low-latitude station of Gadanki.

## 2. Experimental Details

[4] The 18 MHz radar located at Trivandrum is a coherent pulsed Doppler radar and is operated with maximum average power aperture product of $1.25 \times 10^7$ W $m^2$ [*Janardhanan et al.*, 2001]. The MST radar located at Gadanki is a high-power coherent pulsed Doppler radar and is operated with maximum average power aperture product of $7 \times 10^8$ W $m^2$ [*Rao et al.*, 1995]. The system specifications and other important parameters used for the above study are given in Table 1. The sensitivity of the 18 MHz radar is ~24 dB less than that of the 53 MHz radar.

[5] Figures 1a and 1b show the geographic locations and magnetic field line geometry connecting the *F* region over the two locations respectively. It may be noted that the height difference for a particular field line connecting the two locations at the *F* region altitudes is about 100 km. While the dip angle as a function of height remains the same at Trivandrum, it increases from 13.5° at 250 km to 16.1° at 600 km altitude at Gadanki. Accordingly, the radar beam at Trivandrum is oriented vertically, whereas the radar beam at Gadanki is oriented at 14.8° zenith angle due magnetic north in order to satisfy the field perpendicularity condition for detecting the field aligned echoes

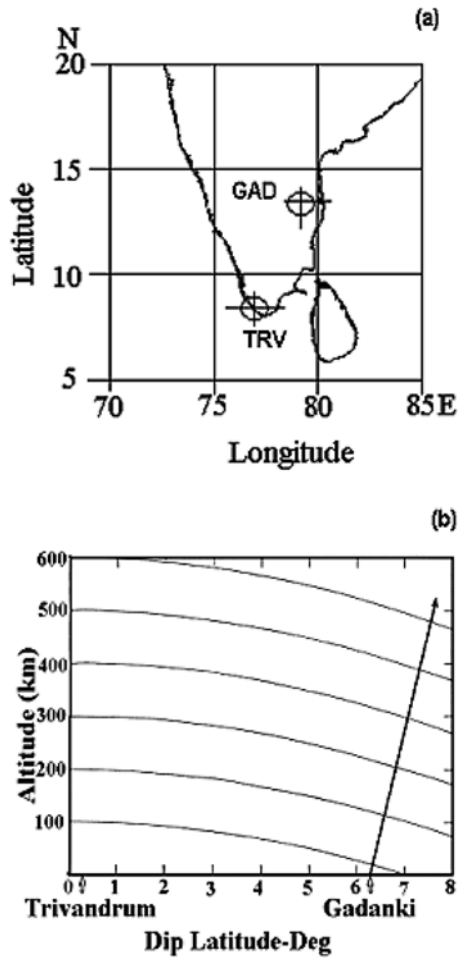


**Figure 1.** (a) Geographic locations and (b) magnetic field geometry for the two radar stations, Trivandrum and Gadanki.

associated with ESF. Because of the finite beam width (half power full beam width = 2.8°) of the Gadanki radar beam, it could satisfy the perpendicularity condition to the magnetic field lines for the height region of our interest. The efficiencies, however, are different at different altitudes.

[6] At both the locations, power spectra were computed online and stored for post processing. In off-line, the three lower-order moments representing total signal power, mean Doppler frequency and spectral width were computed through moments method [*Woodman*, 1985]. Signal-to-noise ratio (SNR) was computed with the noise power reckoned over the entire Doppler window. The observational Doppler windows were ±50 Hz and ±125 Hz for Trivandrum and Gadanki respectively. The spectral width presented here represents the RMS full width ($2\sigma$) of the spectrum.

## 3. Observations and Discussion

### 3.1. Intensity Map

[7] Height-time-intensity (HTI) maps of 12 ESF events observed during March–April 1998 and 1999 at Trivandrum and Gadanki are presented in 12 panels in Figure 2. The top and bottom subpanels in each panel represent HTI maps corresponding to Trivandrum and Gadanki respectively. The continuous and dashed lines plotted in the top subpanels represent the observed virtual height of *F* layer (h′F) prior to the occurrence of spread *F* and bottom height of the *F* region ionogram trace during spread *F* respectively at Trivandrum. The geomagnetic condition in terms of *Ap* index is also given in each panel. Most of the events presented here correspond to magnetically quite condition except those observed on 25 March and 20 April 1998 and 10 and 19 April 1999, which correspond to moderately disturbed conditions. The gray codes in the intensity maps represent SNR. SNR observed at Trivandrum in general is less than that at Gadanki except on 30 March 1998. The stronger signals are associated with topside ESF at both the locations and maximum SNR observed are 40 dB and 45 dB above the 0 dB detectability level at Trivandrum and Gadanki respectively. Cosmic noise at 18 MHz is about 10 times higher than that at 50 MHz. It may be mentioned that the sensitivity of the Trivandrum radar is about 23 dB less than that of Gadanki in terms of average transmitter power and antenna gain. When these factors (cosmic noise, average transmitter power and antenna gain) are considered, SNR observed at Trivandrum appears to be significantly higher (∼25 dB) than that observed at Gadanki.

[8] While the echoes at Trivandrum were observed at altitudes as high as 800 km, they were confined to less than 600 km altitude at Gadanki. The height difference corresponding to the same field lines at the *F* region for the two locations should be about 100 km. Echoes not observed at altitudes greater than 600 km is due to diminishing sensitivity of the Gadanki radar beam as a function of altitude due to the variation of dip angle and very low aspect angle of the 3 m irregularities (<0.015°) [*Farley and Hysell*, 1996]. The occurrence times of ESF irregularities at the two locations are found to agree quite well. On some occasions, echoes have been observed at Trivandrum a little earlier than at Gadanki, but these echoes correspond to bottom-type irregularities. Since Gadanki is only 2°E of Trivandrum (which corresponds to 8 min local time difference), ESF irregularities, except those occurring at lower altitudes, are expected to be observed at Gadanki almost at the same time since they map along the field lines as they grow in height.

[9] There are several differences in terms of the structures. For example, the topside irregularities at Gadanki are characterized by multiple periodic plume structures, whereas at Trivandrum, they are not so. The amplitude spectra of SNR variations (figures not presented) show that the dominant periodicities at Gadanki are in the range of 30–60 min. However, no significant variations in SNR have been observed at Trivandrum. Further, the occurrence of high-altitude plume structures after ∼21 LT and the irregularities, in general, after 23 LT are very infrequent at Trivandrum. Similar observations have been reported by *Tiwari et al.* [2004]. In contrast, irregularities extending to higher altitudes are observed at Gadanki on quite a few occasions even after midnight.

[10] In order to account for the differences in the structures, there are three important factors that need to be taken into account: (1) the sensitivities, (2) the operating frequencies (in terms of irregularity scale size) and (3) the antenna beam widths of the two radars. It is also known that the HTI images are not the true representations of the spatial structures of the unstable ionosphere because of the single slit camera nature of a fixed beam radar [*Woodman and LaHoz*, 1976]. A single slit camera would give a good picture if the target is rigid and moves across the radar beam at a uniform speed and also if the slit is much narrower than all features of the target. However, such conditions are not satisfied for any dynamical phenomenon in the atmosphere in general and more specifically for ESF. Accordingly, the larger beam width of the Trivandrum radar as compared to that of Gadanki would result into more smearing of the structures observed there as compared to that at Gadanki.

[11] The structural differences of the ESF in general at the equator over Jicamarca and at low latitudes like Kwajalein and Gadanki have been well documented in the literature. While at Jicamarca, only limited number of plumes are observed [*Woodman and LaHoz*, 1976; *Hysell and Burcham*, 2002], at Kwajalein as well as at Gadanki, they are many [*Hysell et al.*, 1994; *Rao et al.*, 1997]. The recent results on spread *F* irregularities from Equatorial Atmospheric Radar (EAR), located in West Sumatra, Indonesia (10.36°S dip latitude), also show similar features [*Fukao et al.*, 2003, 2004]. *Hysell et al.* [1994] observed many plume structures associated with spread *F* (as high as 11 in number) at Kwajalein (6.5° dip) in the Pacific sector. The dominant periodicity observed by them was ∼ 30 min. It may be mentioned that at Jicamarca, the occurrence probability of bottom type and bottom side together is about 50%. The rest 50% is mainly topside spread *F* irregularities, which are mainly plume [*Hysell and Burcham*, 2002]. Although such a statistics is not available for Kwajalein and Gadanki, the existing database clearly suggests that the occurrence percentage of plumes is more than the bottom-type and bottom-side structures. All these observations, however, correspond to radar frequencies close to 50 MHz. While there could be some difference due to different radar frequencies and parameters used, the observations brings out the structural differences in the spread *F* irregularities at and off the magnetic equator and this feature seems to

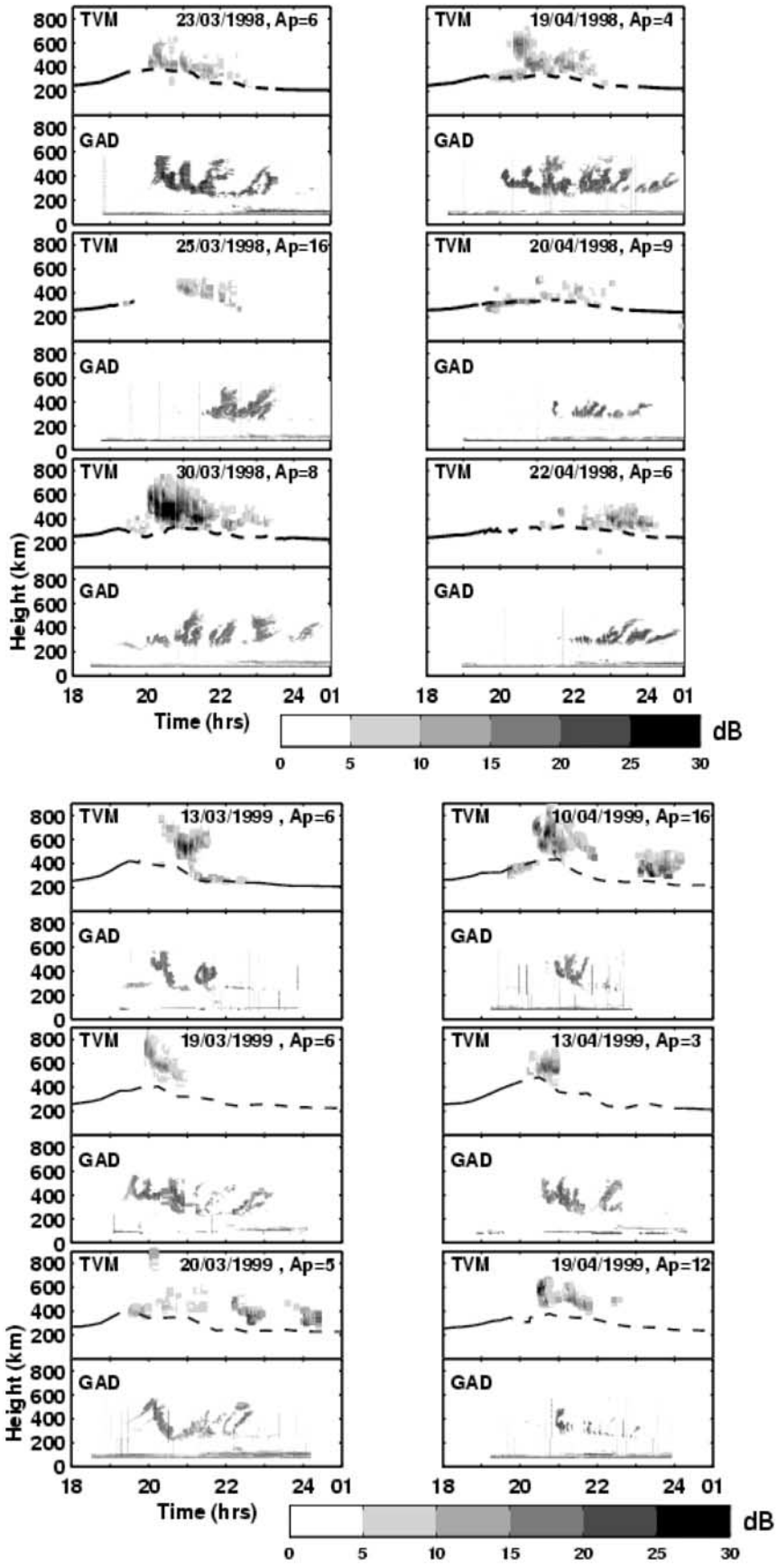


**Figure 2.** Height time intensity plots of 12 events observed at Trivandrum (TVM) and Gadanki (GAD). Dates and the magnetic activities (*Ap* values) are mentioned on each panel.

be consistent with that observed elsewhere. Why multiple plume structures are observed at low latitudes in contrast to that at the magnetic equator is an open issue to be understood.

[12] Another aspect is the infrequent occurrence of 18 MHz observations after 23 LT. In addition, after 21 LT, the high-altitude irregularities are also not observed suggesting that they must be weaker than that of the bottom-side irregularities. The late night topside spread *F* observed at 50 MHz at Jicamarca shows that they are as strong as or stronger than the bottom-side irregularities. They have been observed at Gadanki also. The present database as well as that reported by *Tiwari et al.* [2004] suggests that the postmidnight 8.3 m spread *F* irregularities possibly are too weak to be detected by the existing 18 MHz radar at Trivandrum. In this context, the observations on ESF irregularities reported by *Clemesha* [1964] using a 18 MHz radar and by *Kelleher and Skinner* [1971] using a 27.8 MHz radar are relevant. *Kelleher and Skinner* [1971] have compared their observations with that of *Clemesha* [1964] and have shown that while echoes are observed at 27.8 MHz during 1830–0230, they are observed only during 1830–0000 at 18 MHz. They have also shown that the overall occurrence of echoes is 78% at 27.8 MHz as compared to only 54% at 18 MHz. The observations seem to suggest that the echoes are observed for longer period at higher radar frequency with reference to 18 MHz. The observations presented here are very much consistent with this fact. Further simultaneous observations of ESF with multifrequency radar having similar sensitivity and geometry are essential to understand this aspect satisfactorily.

### 3.2. Doppler Velocity

[13] The Doppler velocities observed over the two locations corresponding to ESF events shown in Figure 2 are presented in Figure 3. The Doppler velocities are both upward and downward and vary with height and time at both the locations. The Doppler velocities corresponding to Trivandrum are in the range of $-100$–$150$ m s$^{-1}$ whereas they are in the range of $-100$–$250$ m s$^{-1}$ at Gadanki. These values are quite similar to that reported earlier by *Sekar et al.* [2000].

[14] In order to make a detailed comparison, the Doppler velocities of the irregularities as a function of time observed at the two locations are plotted side by side in Figure 4a corresponding to 4 selected altitudes. The velocities are also plotted in the form of histogram (normalized occurrence probability distribution function) in Figure 4b to show their distribution. The heights are 405, 450, 495 and 555 km corresponding to Trivandrum and 300, 348, 396 and 449 km corresponding to Gadanki. These heights correspond to the same field lines and hence have been taken for comparison. In Figure 4b the velocities observed at Trivandrum are in the range of $-100$–$150$ m s$^{-1}$ whereas they are in the range of $-100$–$250$ m s$^{-1}$ at Gadanki. The distributions of velocities show that they are of the same order (within $\pm 50$ m s$^{-1}$) although the occurrence distribution is somewhat wider at Trivandrum than that at Gadanki. The occurrence of higher velocities ($>100$ m s$^{-1}$) at Gadanki, although observed infrequently, is relatively more than that over Trivandrum. It may also be mentioned that the amplitudes of different periods of the velocity fluctuations (figures not presented) observed are much higher at Gadanki (20–35 m s$^{-1}$) than that at Trivandrum ($<10$ m s$^{-1}$).

[15] In general, some difference in the velocities could be expected if the measurements are made with radars having different pulse width and beam width. Larger pulse width and beam width can have smearing effects and hence result in somewhat smaller mean velocities. In such a case, spectral width is also expected to be larger corresponding to the measurements made with larger beam width and pulse width. The observations on spectral width presented in the next section, however, do not show such result and hence rules out the contribution of beam width and pulse width effects on the velocities as well.

[16] *Hysell et al.* [1994] observed Doppler velocities equal to several hundred or even more than 1000 m s$^{-1}$ in association with upwelling regions as seen in the intensity map. On one occasion, they observed 1200 m s$^{-1}$, which corresponds to a zonal electric field of more than 30 mV m$^{-1}$. Electric field as large as 50 mV m$^{-1}$ has been observed in the topside plasma depletion through satellite observations [*Aggson et al.*, 1992]. Majority of the velocities observed, however, are within $\pm$100m s$^{-1}$ [*Woodman and LaHoz*, 1976; *Hysell et al.*, 1994; *Patra et al.*, 1997; *Rao et al.*, 1997]. Recent observations made using Equatorial Atmospheric Radar (EAR) [*Fukao et al.*, 2003] also show velocities mostly within $\pm$100 m s$^{-1}$ and occasionally reaching a level of 200 m s$^{-1}$. The velocities observed at both the locations including that made using EAR are comparable and it appears that these observations are in contrast with that reported to be much higher value reaching occasionally supersonic speed at Jicamarca and Kwajalein.

[17] We are aware that these velocities could not be measured unambiguously at 50 MHz using the single pulse technique [*Sahr et al.*, 1989]. For example, for unambiguous measurement of the irregularities at a height of 600 km, the interpulse period should be 4 ms for the equatorial geometry and this will fix the unambiguous velocity limit at $\pm$125 Hz, which corresponds to $\pm$375 m s$^{-1}$ for a 50 MHz radar. Further, the irregularities are overspread for VHF [*Hysell et al.*, 1994] and hence pose serious limitation in measuring the irregularity velocities unambiguously. It may be mentioned that one of the basic ideas for setting up the radar at lower frequency than at 50 MHz is to unambiguously observe the enhanced motion (supersonic flow) associated with ESF irregularities [*Aggson et al.*, 1992]. To our surprise we have not observed velocities exceeding 200 m s$^{-1}$ at Trivandrum in the 12 events shown here and in the observations reported by *Tiwari et al.* [2004]. Numerous examples of 50 MHz radar observations from the equatorial station of Jicamarca are available in literature and show velocities much higher than that measured using 18 MHz radar reported here.

[18] Although Doppler velocities associated with ESF irregularities have been observed extensively by the coherent VHF radars, there is no theory as yet that could relate these to physical parameters. There have been a number of studies aimed at understanding the vertical motion of plasma bubbles [*Ott*, 1978; *Ossakow and Chaturvedi*, 1978; *Anderson and Haerendel*, 1979]. *Ott*

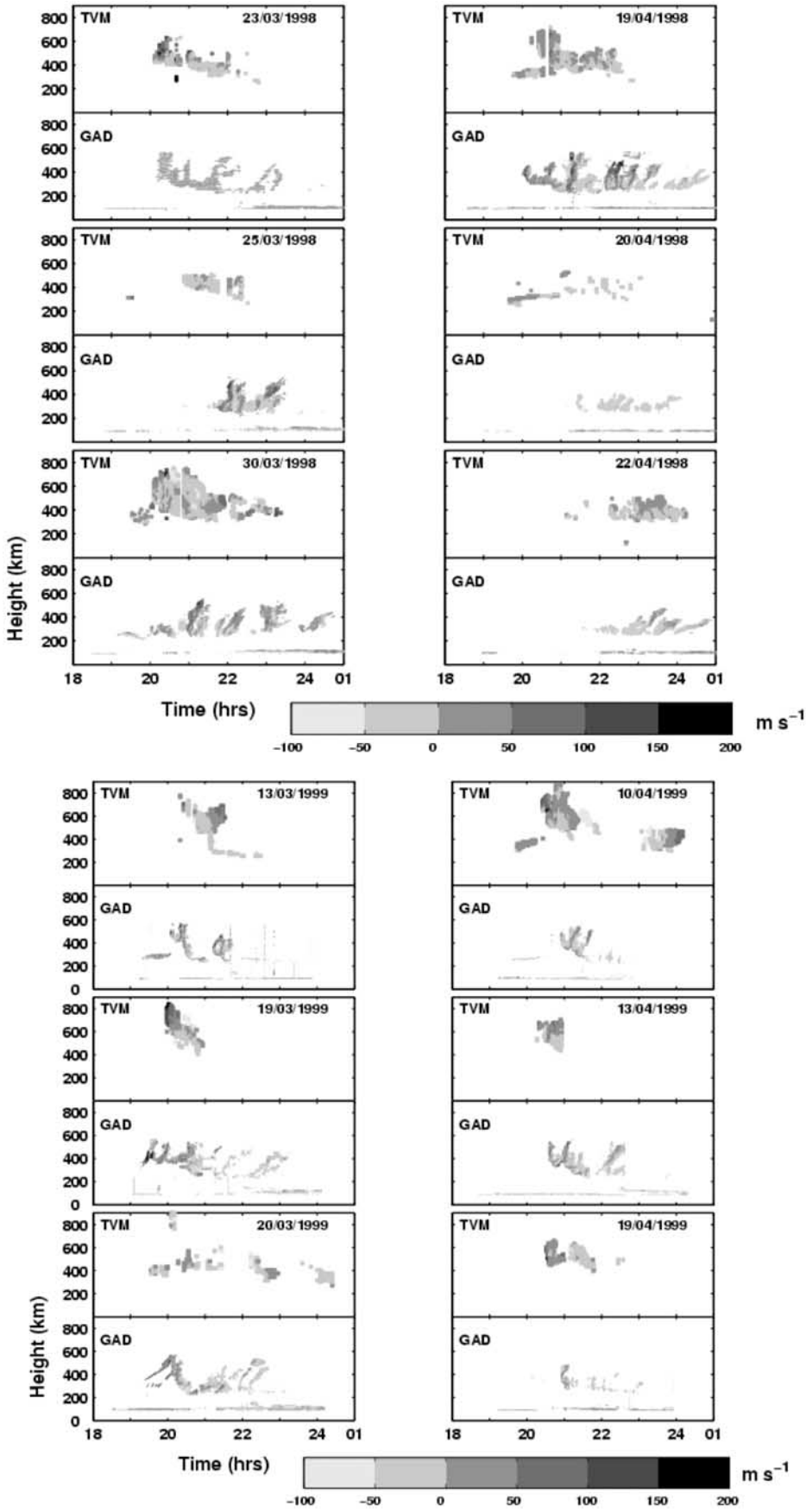


**Figure 3.** Height time velocity maps of the 12 events corresponding to Figure 2. See color version of this figure in the HTML.

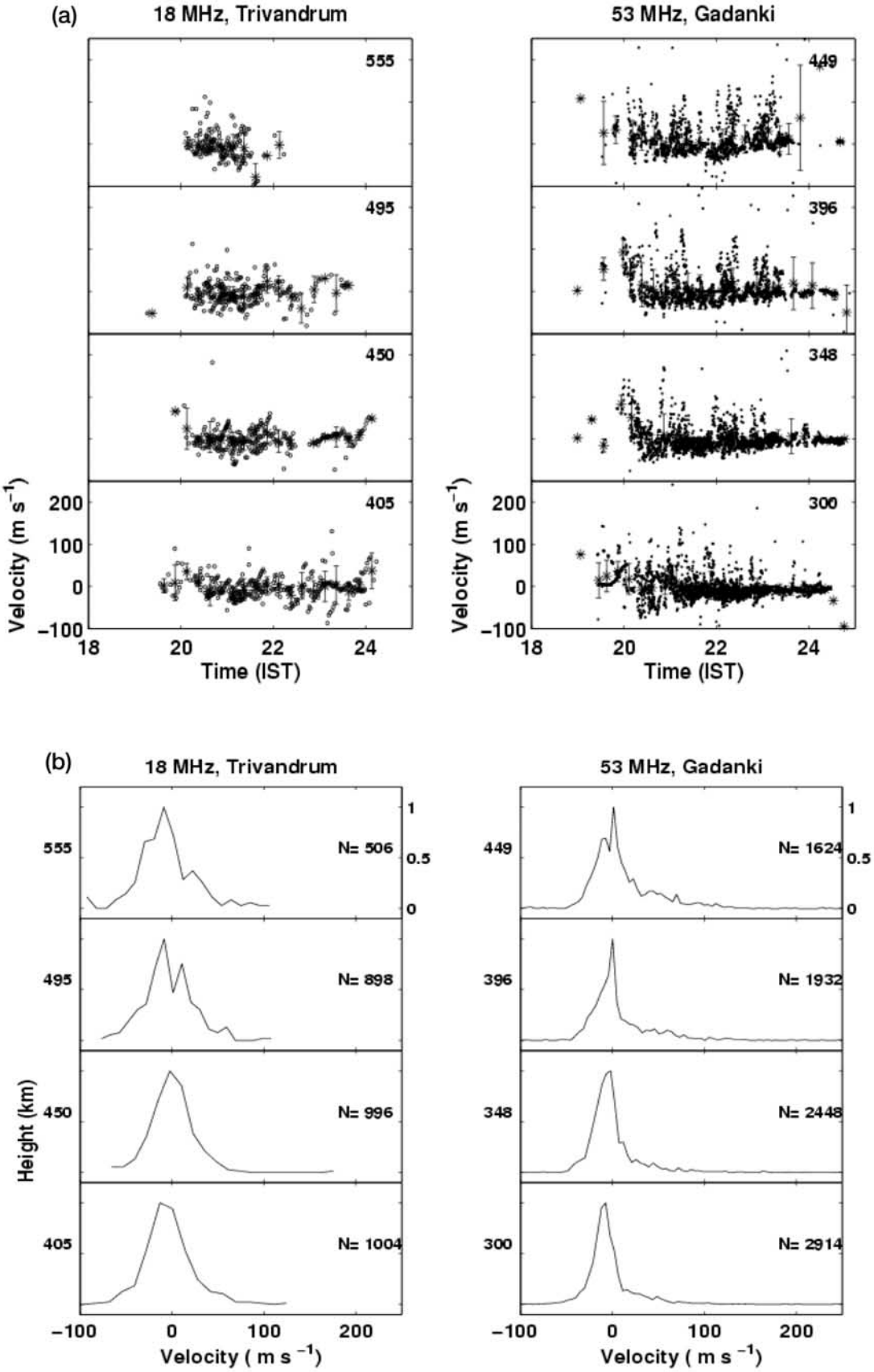


**Figure 4.** (a) Velocities observed at (left) Trivandrum and (right) Gadanki as a function of time for four different heights corresponding to common flux tube. Vertical bars represent standard deviation at 15 min interval. (b) Velocities plotted in the form of histogram corresponding to that shown in Figure 4a.

[1978] described the bubble velocity in both collisional and inertial regimes and provided velocity expressions for particular bubble shapes. The bubble velocity applied to both the regimes has been given as:

$$V = \frac{1}{8}R\left[\left(\nu_{in}^2 + \frac{16g}{R}\right)^{1/2} - \nu_{in}\right]\left[\frac{\Delta n}{n_o + n_1}\right] \quad (1)$$

Where g is the acceleration due to gravity; $\nu_{in}$ is the ion-neutral collision frequency; $n_o$ is the background electron density; $n_1$ is the electron density inside the bubble; $\Delta n = (n_o - n_1)$ and R is the radius of the bubble. The bubble velocity for collisional and inertial case has been shown to be $g/\nu_{in}$ and $0.5(Rg)^{1/2}$. *Ossakow and Chaturvedi* [1978] have shown that the velocity in (1) can be increased by including the elliptical shapes of the bubble that are elongated in the vertical direction. In this case the nonlinear bubble rise velocity is given as:

$$V = \left[\frac{g}{\nu_{in}} + V_0\right]\left[\frac{a\frac{\Delta n}{n_0}}{b + a\left(1 - \frac{\Delta n}{n_0}\right)}\right] \quad (2)$$

Where a and b are the vertical and horizontal dimensions of the bubble respectively and $V_o$ is the background vertical plasma drift. As the axial ratio increases, the bubble velocity approaches the solution for one-dimensional geometry and can become arbitrarily large in the case of strong depletion. *Hysell et al.* [1994] have shown that the plasma advection speed implied for both regimes depends on the ratio of the ambient to depleted densities ($n_o/n_1$) and in one-dimensional case can be written as:

$$V = V_0 + \left(\frac{n_0}{n_1} - 1\right)\left(V_0 + \frac{g}{\nu_{in}}\right)(1 - e^{-\nu_{in}t}) \quad (3)$$

They have shown that the expression of bubble velocity given in (3) is capable of predicting supersonic velocities observed close to the bottom of the channel near the *F* peak.

[19] Using simultaneous radar and rocket-borne observations, *Hysell et al.* [1994] made a detailed investigation on the interpretation of the radar observations. They found that the plasma drift corresponding to the electric field measurements by the rocket probe agrees closely with the Doppler velocities. According to them, the statistics of the coherent radar backscatter at 3-m-scale are controlled by the electrons, which $\mathbf{E} \times \mathbf{B}$ drift under the influence of a spectrum of electric fields and become structured through nonlinear convective steepening. They interpreted that the coherent radar echoes from the *F* region are due mainly to steepened structures, and the Doppler spread of the echoes is due to the advection of the structures. They observed supersonic velocities on quite a few occasions, which were shown to be consistent with simultaneous rocket observations and prediction given by (3). They suggested that rapid $\mathbf{E} \times \mathbf{B}$ plasma advection in spread *F* results from intense electric fields that arise to maintain divergence free current and charge neutrality in the presence of sharp density gradients. Since the diamagnetic drift velocities, even in the region of the sharpest density gradients in spread F, is not expected to approach supersonic speeds, the interpretation offered by them in terms of steepened structures is the most logical one.

[20] In the light of the above discussion, if we were to interpret the radar observations in terms of plasma advection speed in the depletion channel, then the observations seem to suggest that advection speed observed at both the locations are quite similar except for some minor differences. It is quite possible that this difference is due to the two radar frequencies used at the two locations. With the present database, however, it seems difficult to resolve this aspect. What appears to be more important from the observations is that the advection speed observed here is remarkably less than that reported from Jicamarca and Kwajalein. We have also not come across supersonic velocity so far in contrast to that observed over Jicamarca and Kwajalein. If the dimensions of the bubble and degree of depletion are considered to be identical, then the governing factor responsible for the advection speed in equations (2) and (3) is essentially the background vertical plasma drift $V_o$. It may be mentioned that the background vertical plasma drift in the Indian sector is about half of that observed in the American sector [*Hari and Krishna Murthy*, 1995]. Accordingly, the observed lower velocity in the Indian sector than that in the American sector can be understood when different background plasma drifts prevailing in the two sectors are taken into account in equations (2) and (3). The fact that supersonic velocity is not observed in the Indian sector is also consistent with the theoretical expectation based on equation (3).

### 3.3. Spectral Width

[21] Figures 5a and 5b show the spectral width as a function of time and in the form of histogram respectively for the four altitudes shown in Figures 4a and 4b. The spectral widths observed at 18 MHz are found to be less than 100 m $s^{-1}$, whereas they are as high as 300 m $s^{-1}$ at 53 MHz. *Woodman and LaHoz* [1976] measured spectral width ranging from a few meter per second to more than 600 m $s^{-1}$ at Jicamarca. *Balsley et al.* [1972] measured spectral width as high as 600 m $s^{-1}$ from Trivandrum. While, spectral widths observed at Jicamarca, Trivandrum and Gadanki with radars operating at ~50 MHz are quite similar to each other, the same observed with 18 MHz radar reported here are less than 100 m $s^{-1}$.

[22] *Balsley et al.* [1972] and *Woodman and LaHoz* [1976] interpreted the wider spectra in terms of superposition of narrow simpler spectra. *Hysell et al.* [1994] interpreted that the Doppler spread of the echoes is due to the advection of the steepened structures. Unfortunately, since the work of *Woodman and LaHoz* [1976], no major effort has been made to relate the spectral width with any of the physical processes or parameters. Spectral broadening is manifested due to the lifetime of the irregularities and the spatial distribution of velocities representing large-scale dynamics (measured using small-scale scatterers as tracers). Radar observed spectral width, however, is contributed also by nonturbulent component due to the

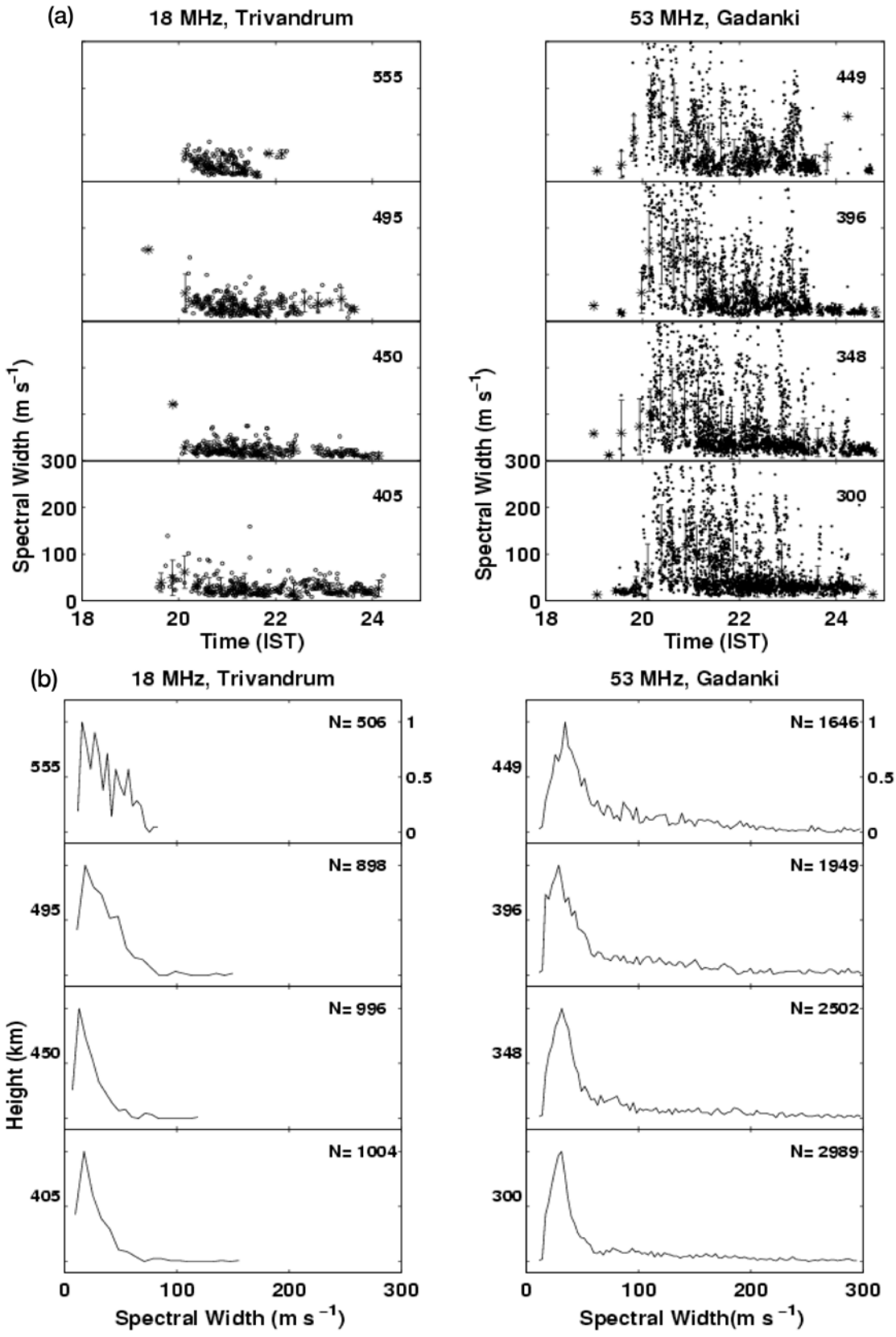


**Figure 5.** (a) Spectral width observed at (left) Trivandrum and (right) Gadanki as a function of time for four different heights corresponding to common flux tube. Vertical bars represent standard deviation at 15 min interval. (b) Spectral width plotted in the form of histogram corresponding to that shown in Figure 5a.

finite volume encompassed by the radar. This, however, does not seem to be important as indicated by the observations. If we believe that the spectral width is mainly controlled by the dynamics of large-scale structures, then the observations suggest different dynamical features for the two locations. While this could be one of the contributing factors, simply this cannot account for the vast difference observed. This is also due to the fact that spectral width >100 m $s^{-1}$ was observed at ~50 MHz in the past from Trivandrum [*Balsley et al.*, 1972]. Simultaneous measurements with radars of different frequency but with identical radar parameters viewing the same ionospheric volume are required to address this aspect. This would also resolve the difference observed in Doppler velocity at the two radar frequencies.

## 4. Concluding Remarks

[23] We presented simultaneous observations of ESF irregularities made using a 18 MHz radar at the equator and a 53 MHz radar at off the equator. The observations clearly bring out the morphological differences of the spread *F* structures observed at and off the equator. The off equatorial structures are characterized by multiple periodic plumes, which are missing at the equator. This aspect is consistent with that studied from Kwajalein and West Sumatra [*Hysell et al.*, 1994; *Fukao et al.*, 2004] and needs to be understood in terms of physical processes responsible for different morphology as a function of latitude. Doppler velocities observed at both the locations are comparable except for velocities >100 m $s^{-1}$ for which the occurrence is relatively more at Gadanki than at Trivandrum. Further it appears that the velocities observed at both the locations are in contrast with that reported to be much higher value reaching occasionally supersonic speed at Jicamarca and Kwajalein. Observations show that spectral widths are remarkably more at 53 MHz as compared to that at 18 MHz. The observations presented here suggest that further simultaneous multifrequency radar observations are essential for a clear understanding of the meter-scale irregularities associated with equatorial spread F.

[24] **Acknowledgments.** The 18 MHz radar belongs to and operated by the Space Physics Laboratory, Vikram Sarabhai Space Centre. The 53 MHz MST radar is operated as a national facility under Department of Space, Government of India. We are grateful to the engineering staff at both the centers without whose support the observations presented here would not have been made possible. Authors are thankful to both the reviewers for their valuable suggestions for the improvement of the paper.

[25] Arthur Richmond thanks the reviewers for their assistance in evaluating this paper.

## References

Aggson, T. L., W. J. Burke, N. C. Maynard, W. B. Hanson, P. C. Anderson, J. A. Slavin, W. R. Hogey, and J. L. Saba (1992), Equatorial bubbles updrafting at supersonic speeds, *J. Geophys. Res.*, *97*, 8581.

Anderson, D. N., and G. Haerendel (1979), The motion of depleted plasma regions in the equatorial ionosphere, *J. Geophys. Res.*, *84*, 4251.

Balsley, B. B., G. Haerendel, and R. A. Greenwald (1972), Equatorial spread *F*: Recent observations and a new interpretation, *J. Geophys. Res.*, *77*, 5625.

Basu, S., E. MacKenzie, and S. Basu (1988), Ionospheric constraints on VHF/UHF communication links during solar maximum and minimum periods, *Radio Sci.*, *23*, 363.

Berkner, L. V., and H. W. Wells (1934), *F* region ionospheric investigation at low latitudes, *J. Geophys. Res.*, *39*, 215.

Booker, H. G., and H. W. Wells (1938), Scattering of radio waves by the *F* region of the ionosphere, *J. Geophys. Res.*, *43*, 249.

Chandra, H., et al. (1993), Coordinated multi-station observations in India during March–April 1991, *Indian J. Radio Space Phys.*, *22*, 69.

Clemesha, B. R. (1964), An investigation of the irregularities in the *F*-region associated with equatorial type spread-*F*, *J. Atmos. Terr. Phys.*, *26*, 91.

Farley, D. T., and D. L. Hysell (1996), Radar measurements of very small aspect angles in the equatorial ionosphere, *J. Geophys. Res.*, *101*, 5177.

Fukao, S., H. Hashiguchi, M. Yamamoto, T. Tsunoda, T. Nakamura, and M. K. Yabugaki (2003), The equatorial atmospheric radar (EAR): System description and first results, *Radio Sci.*, *38*(3), 1053, doi:10.1029/2002RS002767.

Fukao, S., Y. Ozawa, T. Yokoyama, M. Yamamoto, and R. T. Tsunoda 2004, First observations of the spatial structure of *F* region 3-m-scale field-aligned irregularities with the Equatorial Atmospheric Radar in Indonesia, *J. Geophys. Res.*, *109*, A02304, doi:10.1029/2003JA010096.

Hanson, W. B., and D. K. Bamgboye 1984, The measured motions inside equatorial plasma bubbles, *J. Geophys. Res.*, *89*, 8997.

Hari, S. S., and B. V. Krishna Murthy (1995), Equatorial night-time *F*-region zonal electric field, *Ann. Geophys.*, *13*, 871.

Hysell, D. L., and J. Burcham (1998), JULIA radar studies of equatorial spread *F*, *J. Geophys. Res.*, *103*, 29,155.

Hysell, D. L., and J. D. Burcham (2002), Long term studies of equatorial spread *F* using the JULIA radar at Jicamarca, *J. Atmos. Sol. Terr. Phys.*, *64*, 1531.

Hysell, D. L., and R. F. Woodman (1997), Imaging coherent backscatter radar observations of topside equatorial spread *F*, *Radio Sci.*, *32*, 2309.

Hysell, D. L., M. C. Kelley, W. E. Swartz, and D. T. Farley (1994), VHF radar and rocket observations of equatorial spread *F* on Kwajalein, *J. Geophys. Res.*, *99*, 15,065.

Janardhanan, K. V., D. Ramakrishna Rao, K. S. Viswanathan, B. V. Krishna Murthy, K. S. V. Shenoy, S. V. Mohan Kumar, K. P. Kamath, K. K. Mukundan, G. Sajitha, M. Shajahan, and C. Ayyappan (2001), HF backscatter radar at the magnetic equator: System details and preliminary results, *Indian J. Radio Space Phys.*, *30*, 77.

Kelleher, R. F., and N. J. Skinner (1971), Studies of *F* region irregularities at Nairobi II—by direct backscatter at 27.8 MHz, *Ann. Geophys.*, *27*, 195.

Kelley, M. C., et al. (1986), The Condor equatorial spread *F* campaign: Overview and results of the large-scale measurements, *J. Geophys. Res.*, *91*, 5487.

Krishnamoorthy, K., C. R. Reddy, and B. V. Krishna Murthy (1979), Night-time ionospheric scintillations at the magnetic equator, *J. Atmos. Terr. Phys.*, *41*, 123.

McClure, J. P., W. B. Hanson, and J. H. Hoffman (1977), Plasma bubbles and irregularities in the equatorial ionosphere, *J. Geophys. Res.*, *82*, 2650.

Ossakow, S. L., and P. K. Chaturvedi (1978), Morphological studies of rising equatorial spread *F* bubbles, *J. Geophys. Res.*, *83*, 2085.

Ott, E. (1978), Theory of Rayleigh-Taylor bubbles in the equatorial ionosphere, *J. Geophys. Res.*, *83*, 2066.

Patra, A. K., V. K. Anandan, P. B. Rao, and A. R. Jain (1995), First observations of equatorial spread *F* from Indian MST radar, *Radio Sci.*, *30*, 1159.

Patra, A. K., P. B. Rao, V. K. Anandan, and A. R. Jain (1997), Radar observations of 2.8 m equatorial spread *F* irregularities, *J. Atmos. Sol. Terr. Phys.*, *59*, 1633.

Pfaff, R. F., J. H. A. Sobral, M. A. Abdu, W. E. Swartz, J. W. Labelle, M. F. Larsen, R. A. Goldberg, and F. J. Schimidlin (1997), The Guara Campaign: A series of rocket-radar investigations of the Earth's upper atmosphere at the magnetic equator, *Geophys. Res. Lett.*, *24*, 1663.

Rao, P. B., A. R. Jain, P. Kishore, P. Balamuralidhar, S. H. Damle, and G. Viswanathan (1995), Indian MST radar: 1. System description and sample vector wind measurements in ST mode, *Radio Sci.*, *30*, 1125.

Rao, P. B., A. K. Patra, T. V. Chandrasekhar Sharma, B. V. Krishna Murthy, K. S. V. Subbarao, and S. S. Hari (1997), Radar observations of updrafting and downdrafting plasma depletions associated with equatorial spread *F*, *Radio Sci.*, *32*, 1215.

Sahr, J. D., D. T. Farley, and W. E. Swartz (1989), Removal of aliasing in pulse-to-pulse Doppler radar measurements, *Radio Sci.*, *24*, 697.

Sekar, R., E. A. Kherani, K. S. Viswanathan, A. K. Patra, P. B. Rao, C. V. Devasia, K. S. V. Subbarao, D. Tiwari, and N. Ramachandran (2000), Preliminary results and equatorial spread *F* irregularities by VHF and HF radars, *Indian J. Radio Space Phys.*, *29*, 262.

Sinha, H. S. S., S. Raizada, and R. N. Misra (1999), First simultaneous in situ measurement of electron density and electric field fluctuations during spread *F* in the Indian zone, *Geophys. Res. Lett.*, *26*, 1669.

Sinha, H. S. S., P. K. Rajesh, R. N. Misra, and N. Dutt (2001), Multi-wavelength imaging observations of plasma depletions over Kavalur, India, *Ann. Geophys.*, *19*, 1119.

Tiwari, D., A. K. Patra, C. V. Devasia, R. Sridharan, N. Jyoti, K. S. Viswanathan, and K. S. V. Subbarao (2004), Radar observations of 8.3 m scale equatorial spread *F* irregularities over Trivandrum, *Ann. Geophys.*, *22*, 911.

Towle, D. M. (1980), VHF and UHF radar observations of equatorial *F* region ionospheric irregularities and background densities, *Radio Sci.*, *15*, 71.

Tsunoda, R. T. (1980), Backscatter measurements of 11 cm equatorial spread *F* irregularities, *Geophys. Res. Lett.*, *7*, 848.

Tsunoda, R. T., M. J. Barton, J. Owen, and D. M. Towle (1979), Altair incoherent scatter radar for equatorial spread *F* studies, *Radio Sci.*, *14*, 1111.

Vickrey, J. F., M. C. Kelley, R. Pfaff, and S. R. Goldman (1984), Low-latitude image striations associated with bottomside equatorial spread *F*: Observations and theory, *J. Geophys. Res.*, *89*, 2955.

Weber, E. J., J. Buchau, R. H. Eather, and S. B. Mende (1978), North-south field aligned equatorial airglow depletions, *J. Geophys. Res.*, *83*, 712.

Woodman, R. F. (1985), Spectral moment estimation in MST radars, *Radio Sci.*, *20*, 1185.

Woodman, R. F., and C. LaHoz (1976), Radar observations of *F* region equatorial irregularities, *J. Geophys. Res.*, *81*, 5447.

C. V. Devasia, R. Sridharan, K. S. V. Subbarao, and K. S. Viswanathan, Space Physics Laboratory, Vikram Sarabhai Space Centre, ISRO, Trivandrum 695 022, India.

E. A. Kherani, Instituto Nacional de Pesquisas Espaciais, Av. dos Astronautas, 1.758 - Jd. Granja, CEP 12227-010, São José dos Campos, SP, Brazil.

A. K. Patra, National MST Radar Facility, Department of Space, P.O. Box 123, Tirupati 517 502, AP, India. (patra_nmrf@rediffmail.com)

P. B. Rao, National Remote Sensing Agency, Department of Space, Government of India, Balanagar, Hyderabad -500 037, India.

R. Sekar, Physical Research Laboratory, Room 653, Navrangpura, Ahmedabad 380 009, India.

S. Sripathi and D. Tiwari, Indian Institute of Geomagnetism, Navi Mumbai 400 005, India.